Remote Sens. **2015**, *7*, 3184-3205; doi:10.3390/rs70303184

OPEN ACCESS

remote sensing

ISSN 2072-4292

www.mdpi.com/journal/remotesensing

Article

Improvement of Soil Moisture Retrieval from Hyperspectral VNIR-SWIR Data Using Clay Content Information: From Laboratory to Field Experiments

Rosa Oltra-Carrió [1,†,*], Frédéric Baup [2,†], Sophie Fabre [1,†], Rémy Fieuzal [2,†] and Xavier Briottet [1,†]

[1] DOTA-ONERA, 2 Avenue Edouard Belin, 31055 Toulouse Cedex 4, France;
E-Mail: sophie.fabre@onera.fr (S.F.); xavier.briottet@onera.fr (X.B.)

[2] CESBIO, 18 avenue. Edouard Belin, 31401 Toulouse Cedex 9, France;
E-Mails: frederic.baup@iut-tlse3.fr (F.B.); fieuzal.remy@neuf.fr (R.F.)

† These authors contributed equally to this work.

* Author to whom correspondence should be addressed; E-Mail: roltra@onera.fr;
Tel.: +33-562-252-608; Fax: +33-562-252-588.

Academic Editors: George P. Petropoulos and Prasad S. Thenkabail

Received: 14 November 2014 / Accepted: 15 February 2015 / Published: 20 March 2015

Abstract: The aim of this work is to study the constraints and performance of SMC retrieval methodologies in the VNIR (Visible-Near InfraRed) and SWIR (ShortWave InfraRed) regions (from 0.4 to 2.5 µm) when passing from controlled laboratory conditions to field conditions. Five different approaches of signal processing found in literature were considered. Four local criteria are spectral indices (WISOIL, NSMI, NINSOL and NINSON). These indices are the ratios between the spectral reflectances acquired at two specific wavelengths to characterize moisture content in soil. The last criterion is based in the convex hull concept and it is a global method, which is based on the analysis of the full spectral signature of the soil. The database was composed of 464 and 9 spectra, respectively, measured over bare soils in laboratory and *in-situ*. For each measurement, SMC and texture were well-known and the database was divided in two parts dedicated to calibration and validation steps. The calibration part was used to define the empirical relation between SMC and SMC retrieval approaches, with coefficients of determination (R^2) between 0.72 and 0.92. A clay content (CC) dependence was detected for the NINSOL and NINSON indices. Consequently, two new criteria were proposed taking into account the CC contribution ($NINSOL_{CC}$ and $NINSON_{CC}$). The well-marked regression between SMC and global/local indices, and the interest of using the CC, were confirmed during the validation step using laboratory data (R^2

superior to 0.76 and Root mean square errors inferior to 8.3% $m^3 \cdot m^{-3}$ in all cases) and using *in-situ* data, where WISOIL, $NINSOL_{CC}$ and $NINSON_{CC}$ criteria stand out among the NSMI and CH.

Keywords: soil moisture content; clay content; WISOIL; NSMI; NINSOL; NINSON; CH

1. Introduction

Meteorological, hydrological and ecological processes are influenced by soil moisture [1]. Indeed, this parameter has a key role in controlling the exchange of water and heat energy between the land surface and the atmosphere through evaporation and plant transpiration [2–4]. It contributes to the hydrologic cycle process, specifically on the partition between runoff and infiltration in arid but also in temperate zones [5]. At the global scale, this will influence the relative contribution between incoming radiation and latent and sensible heat fluxes on the radiative budget [6,7]. At the regional and local scales, Soil Moisture Content (SMC) has an impact on erosion (which leads to soil and organic matter losses), soil contamination, crusting, soil compaction and salinity. These phenomena have an impact on soils and in particular on agricultural soils. Agriculture is facing an increasing impact of anthropogenic activities as a result of a growing human population which does not only affect crop production, but also soil ecosystem services [8,9]. Accurate estimation of SMC with a high spatial resolution would improve the characterization of soil texture like soil organic carbon or clay [10,11] but also the growth of the vegetation [12] and its biodiversity [13]. Timely characterization of soil moisture is widely used in drought analysis [14,15], crop yield estimation [16,17], irrigation management of precision agriculture [18,19], and plant health [20].

Traditionally, methods for monitoring soil moisture (gravimetric, electromagnetic, thermal, *etc.*) [21], are based on site-scale or local survey and do not allow for the characterization of the high spatial and temporal variability at large scale of the SMC [22,23]. Remote sensing techniques can overcome these limitations as they provide better temporal and spatial coverages [24]. Commonly, SMC is estimated from active or passive microwave data due to their high discrimination potential between different soil moisture levels [25,26]. Nevertheless, these data have two main limitations: their high sensitivity to surface roughness [27] for SAR (Synthetic Aperture Radar) sensor and their coarse spatial resolution. However, numerous spectroscopic studies have been conducted to characterize the SMC influence on the spectral reflectance mainly with laboratory and with few *in-situ* measurements [20,28,29]. Angström [30] demonstrated through laboratory measurements that soil moisture content had an impact on the behavior of soil spectral reflectances in the solar domain. This work exhibited a decrease of the reflectance level as SMC increased due to the darkening of the soil surface. Later, other laboratory acquisitions over bare soils [31–33] confirmed this behavior, which has been used to develop SMC approaches from spectral reflectance [34,35]. From these laboratory measurements, models were developed to retrieve the SMC. Most of them are based on calibration models developed to predict soil moisture using Near Infrared (NIR) spectroscopy [36,37]. However, there is a lack of studies applying the laboratory-calibrated models to outdoor datasets. Indeed, this is a difficult task and more work is needed on spectral data comparison between field and laboratory to establish an accurate spectrum-soil

moisture inversion model [20]. In addition, most of the results suggest the need to take into account the factors influencing surface reflectance, such as roughness and texture, organic matter content, vegetation cover and mineral composition [16,38] to improve the performance of the SMC retrieval [27]. One of the most important texture parameter is the clay content (CC). As mentioned by [39], water retention of soil depends on its organic and mineralogical compositions. Their results show that the properties of water retention of clay soil depend on the clay mass, on the organization of the granulometry and finally on the CC.

Nowadays, the advent of new hyperspectral image systems in the 0.4–2.5 μm spectral range is giving a boost to reflectance-based techniques to estimate the SMC [40]. These approaches seem to be less sensitive to surface roughness than microwave imagery and offer richer spectral information than traditional multispectral system. The main limitations of the hyperspectral imagery are related to the representation of the ground surface (no soil penetration), to their dependence on weather conditions, which need substantial atmospheric correction to retrieve surface reflectance, and to the signal noise ratio of the sensor [40]. Despite these drawbacks, there is a real interest to estimate the SMC from such sensors [41]. Several papers describe soil surface moisture estimation using airborne data [42–45]. Haubrock *et al*. [46] show a clear connection between their image based data retrieved by using the Normalised Soil Moisture Index (NSMI) and *in-situ* measurements of top layer soil moisture. These results encourage the community in considering the future hyperspectral space missions to retrieve the SMC from space remote sensing. PRISMA (Hyperspectral Precursor of the Application Mission) [47], and EnMAP (Environmental Mapping and Analysis Program) [48] are two VNIR (Visible-Near InfraRed) and SWIR (ShortWave InfraRed) hyperspectral instruments that will be, respectively, launched in 2015 and 2018, and HYPXIM (HYPerspectral IMagerie) [49] sensor is planned to be operative before 2025. These missions will cover the reflective domain from 0.4 μm to 2.5 μm with a 10 nm spectral resolution. Specifically, the combination of high spectral resolution with a high spatial resolution, better than 10 m in the HYPXIM case, opens the way to the monitoring of the soil moisture dynamic for the development of precision agriculture [20].

The present study focuses on examining the potential of hyperspectral data (from 0.4 μm to 2.5 μm) to retrieve soil moisture content, by taking into account the soil CC, and when passing from controlled laboratory conditions to field conditions. In this work, *in-situ* data were collected over agricultural plots. Laboratory data were achieved by the French spatial laboratory ONERA. Data come from two experiments conducted in 2010 and 2013 [50]. The paper is organized as follows: The study site and the associated data collection (soil moisture, texture and spectral signature) are presented in Section 2. The methodology is explained in Section 3, presenting global and local criteria used to retrieve SMC from reflectance spectrum. Section 4 presents the results of the calibration and validation steps for soil moisture retrieval, considering laboratory and *in-situ* data. Conclusions and Perspectives are given in Section 5.

2. Study Site and Data Collection

2.1. Site Description

The study site is located in southwestern France, near Toulouse (Figure 1a,b). It has been instrumented with two meteorological stations near to the villages of Lamasquère and Auradé (Figure 1c,d).

Climatic stations collect soil moisture, air and soil temperatures, radiative and energy fluxes, in the framework of the "Sud Ouest" project of the CESBIO laboratory [51,52].

The region is governed by a temperate climate, with annual amount of rainfall close to 600 mm, and maximal mean daily air temperature near 25 °C in summer. The study area is highly anthropized, and the surfaces are mainly dedicated to agricultural activities (90% of the landscape). It is oriented towards polyculture/livestock, and is composed of crops (56.8%), forests (7.9%), urban areas (2.4%), grasslands (32.1%) and water bodies (0.8%). In this region of alluvial plains and hills, the steepest slopes never exceed 13.4° [53].

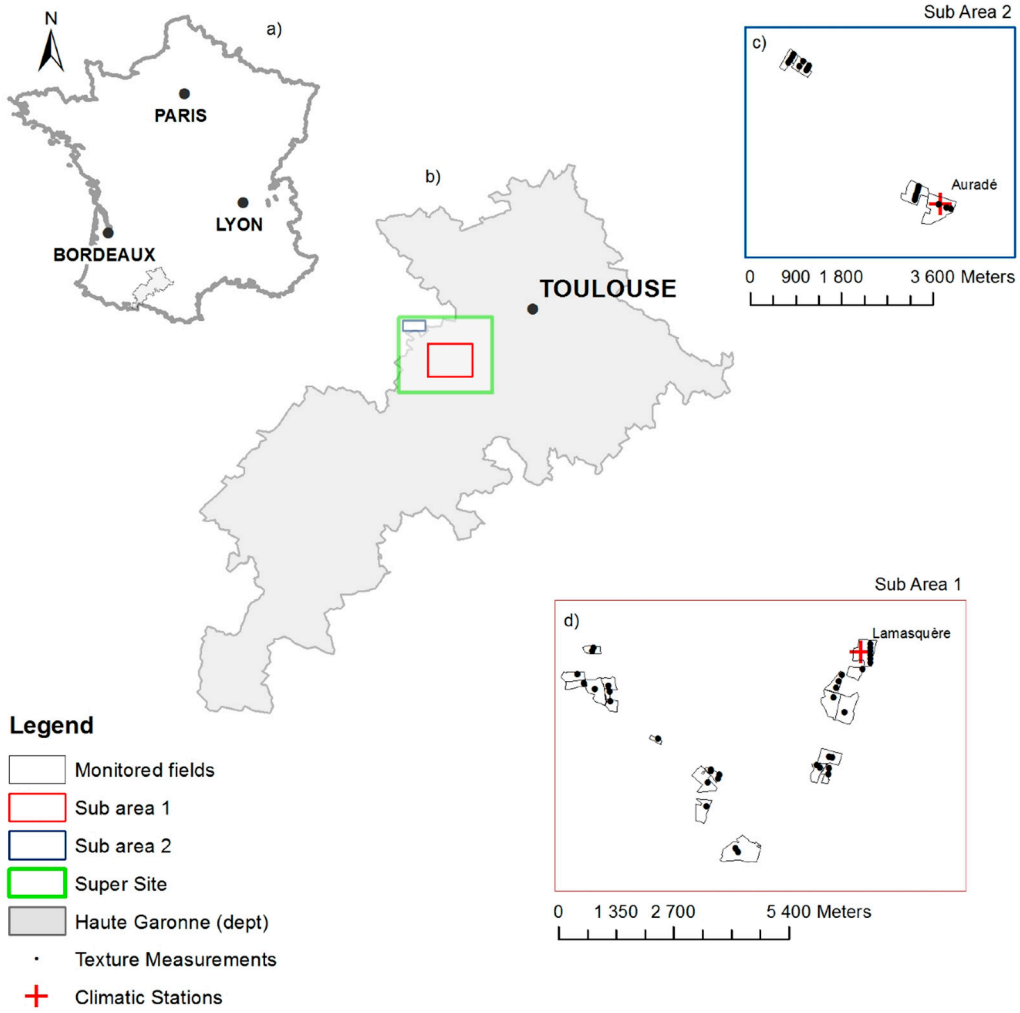

Figure 1. The studied site is located in the southwestern France, in the department of Haute Garonne (**a**), including two sub-areas named "Lamasquère" (red empty rectangle) and "Auradé" (blue empty rectangle) (**b**–**d**). Texture measurements are shown as black dots, within the agricultural plots (c and d).

2.2. Soil Moisture Content

2.2.1. Laboratory Data

The measurement process in the laboratory was based on the experimental protocol described in [33]. The soil sample was humidified until saturation. Then, eight or nine different levels of SMC

(depending on the sample) were artificially obtained by progressively drying the sample in a laboratory oven. The oven was warmed up to a fixed temperature of 60 °C, which avoids any crack in the surface of the sample. Each level of SMC was achieved after 35 min of oven drying and the sample was considered as completely dried after 24 h in the oven. Soil samples were weighed, with a high precision balance (0.1 mg), at the saturation level and after each drying step.

The SMC levels of the reference database from laboratory measurements were quantified by a gravimetric method [37]:

$$\mathrm{SMC}_g = \frac{m_w - m_d}{m_w} \times 100 \quad (1)$$

where SMC_g represents the gravimetric SMC, m_w is the mass of the wet sample at a given drying stage, and m_d is the mass of the completely dried sample.

Then, the volumetric SMC was obtained according to Equation (2) [36]:

$$\mathrm{SMC}_v = \mathrm{SMC}_g \frac{d_w}{d_{\mathrm{water}}} \quad (2)$$

where d_{water} is the water density (d_{water} = 1 g·cm^{-3}) and d_w is the wet sample density:

$$d_w = \frac{m_w}{V_w} \quad (3)$$

where V_w is the volume of the wet sample, defined as the difference between the volume of the sample in the saturation moment (V_{sat}) and the volume of water removed during the drying process (V_{water}) (Equation (4)).

$$V_w = V_{\mathrm{sat}} - V_{\mathrm{water}} \quad (4)$$

At the saturation moment the sample filled all the recipient, so V_{sat} was equivalent to the recipient volume. The V_{water}, is given by Equations (5) and (6).

$$V_{\mathrm{water}} = \frac{m_{\mathrm{water}}}{d_{\mathrm{water}}} \quad (5)$$

$$m_{\mathrm{water}} = m_w - m_d \quad (6)$$

2.2.2. *In-situ* Data

A mobile Delta-T Theta Probe sensor (ML2x) was used to measure *in-situ* volumetric soil moisture content with a penetration in the soil of 5 cm [54]. The mobile sensor was calibrated using gravimetric measurements performed during the Multisensors Crop Monitoring Experiment (MCM'10) conducted in 2010 [50], obtaining a coefficient of determination (R^2) equal to 0.83 and root mean square errors (RMSE) lower than 3% m^3·m^{-3}.

2.3. Clay Content

The 57 soil texture measurements are presented in the Figure 2. For each measure, the field-collection consisted in sampling the surface (0–25 cm depth), inside a circle of 10 meters radius, with 16 sub-samples [50]. The measurements filled three classes of the European Soil Map (HYPRES) texture classification system (*i.e.*, Fine, Medium and Medium Fine) [55], with contents in clay, silt and sand

ranging, respectively, between 10% and 57%, 22% and 77%, 4% and 53%. The soils were dominated by the content in silt, as shows the mean value of 47%, followed by the fraction of clay (29.7%) and sand (23.3%). These results highlight the wide range of sampled soil texture (which are representatives of the study area).

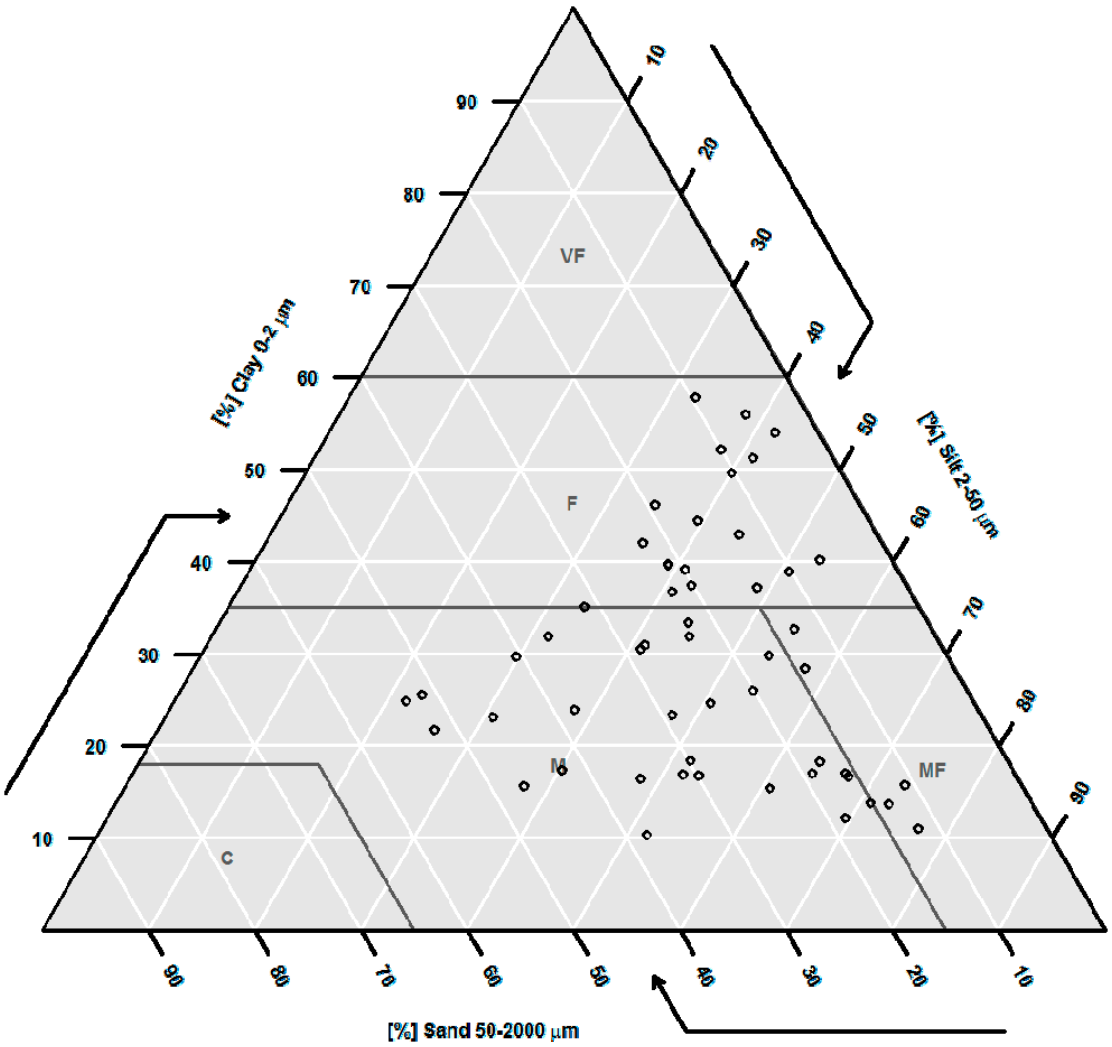

Figure 2. Distribution of the 57 soil texture measurements inside the textural triangle as defined by the European Soil Map (HYPRES) texture classification system. The triangle is divided in five classes: Very Fine (VF), Fine (F), Medium Fine (MF), Medium (M) and Coarse (C).

2.4. Spectral Signatures

Laboratory and *in-situ* soil spectral reflectance measurements were performed using an ASD (Analytical Spectral Device) FiledSpec Pro FR spectroradiometer. This portable instrument measures conical spectral reflectance with a 0.35–2.50 µm spectral range using three detectors. The VNIR portion of the spectrum (0.35–1.00 µm) is measured by a 512-element silicon photodiode array. The SWIR spectral range (1.00–2.50 µm) is acquired with two separate thermo-electrically cooled indium gallium arsenide (InGaAs) detectors. Spectral specifications of this device are listed in Table 1.

Table 1. ASD FieldSpec Pro specifications.

	Spectral Range	Spectral Resolution	Spectral Sampling
VNIR	0.35–1.00 μm	3 nm at 0.70 μm	1.4 nm (0.35–1.05 μm)
SWIR	1.00–2.50 μm	10 nm at 1.40 μm 12 nm at 2.10 μm	2 nm (1.05–2.50 μm)

To measure the reflectance of a sample (ρ) the reflectance of a white reference (ρ_{ref}) is required. This latter was obtained with a Spectralon (Labsphere, North Sutton, NH, USA) panel. Finally, after dark current correction, ρ is given by Equation (7).

$$\rho = \frac{L_{\text{sam}}}{L_{\text{ref}}}\rho_{\text{ref}} \tag{7}$$

where L_{sam} is the measured radiance from the sample and L_{ref} is the measured radiance from the white reference.

2.4.1. Laboratory Spectra

The laboratory measurements were performed according to the experimental protocol defined in [33]. The sample was uniformly illuminated by a solar halogen lamp with an illumination zenith angle of 15°. The ASD was used with a field of view (FOV) of 10°, with a nadir observation, and placed at around 20 cm from the sample (see Figure 3). The observed surface had a diameter of 6 cm. The spectral reflectance was measured for each sample at different SMC (see Section 2.2.1) and then the spectra were smoothed with a Savitzky-Golay filter for reducing noisy signal [56].

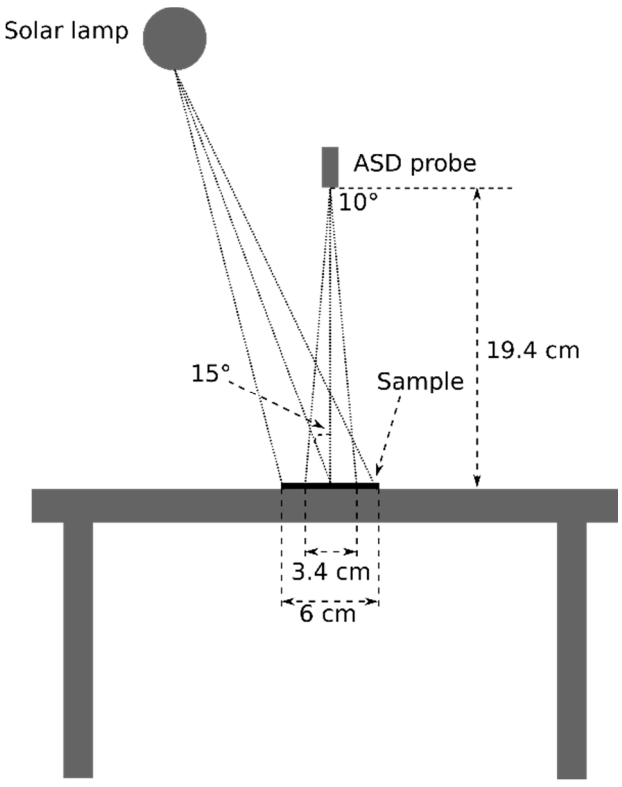

Figure 3. Experimental set-up for soil spectra acquisitions.

The spectral signatures of the 57 bare soil samples characterized by their clay, silt and sand contents were performed for 8 or 9 SMC levels (depending on the sample). A reference database was built from these laboratory measurements, composed of 464 spectral signatures. Figure 4 shows an example of spectral reflectances depending on the SMC (ranged from 0% $m^3 \cdot m^{-3}$ to 48% $m^3 \cdot m^{-3}$), for a soil sample with a CC of 30%, 16% of sand and 54% of silt. Results showed that the reflectance decreased when the SMC increased, as already described in the literature [32,33]. Moreover, water absorption bands around 1.4 µm and 1.9 µm are more noticeable for wettest samples.

2.4.2. *In-situ* Spectra

In-situ spectra measurements were performed close to 12 am (GMT), on 24 April 2013 under sunny conditions, using a mobile ASD. At this date, the soil was prepared for sowing (smooth) and bare, without stubs or any residues. Observation conditions were fixed to be consistent with laboratory measurements (footprint of about 6 cm of diameter). Nine spectra were collected over an irrigated area in the Lamasquère area (see Figure 1). Each *in-situ* spectrum was then smoothed using a Savitzky-Golay filter [56] like in laboratory measurements and the noisy signal in the atmospheric water vapor absorption bands (around 1.4 µm and around 1.9 µm) was removed.

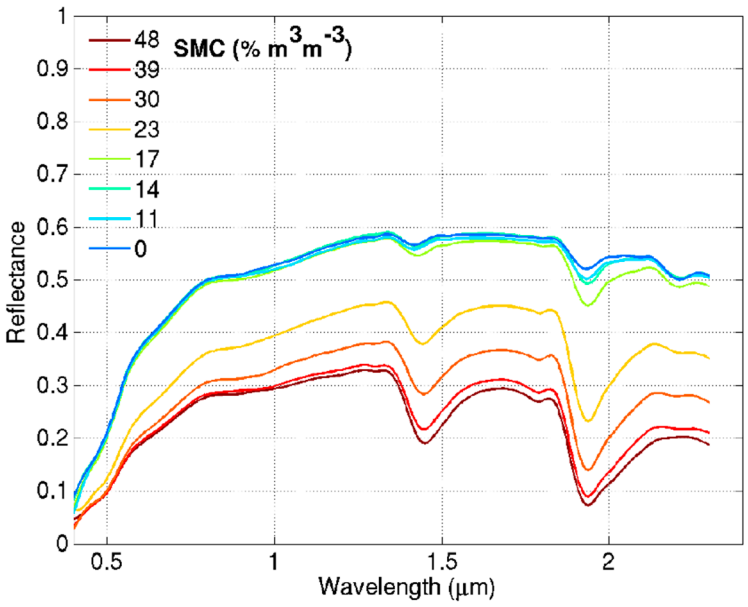

Figure 4. Evolution of the spectral signatures depending on the volumetric soil moisture content ranging between 0 and 48% $m^3 \cdot m^{-3}$. The soil sample is composed with 30% of clay, 16% of sand and 54% of silt.

3. Methodology

The flowchart, presented in Figure 5, summarizes the different steps used to estimate the SMC from spectral information. The spectral signatures, acquired in laboratory or *in-situ*, were used to process four local indices and one global criterion, as detailed in the following Sections (3.1 and 3.2). The SMC estimation was achieved using one calibration and one validation step. The calibration one was used to initialize the parameters of the SMC retrieval models. The calibration database was composed of 50%

of the 464 spectral signatures in the reference dataset and their related SMC data. The validation process was performed using both the other 50% of the reference dataset, and 9 *in-situ* data (spectra and associated SMC). The division of the entire database in two datasets ensured an equal distribution of the samples covering the same SMC range in both cases. In the validation step, we also evaluated the interest of using the CC information to improve the SMC estimation. Results were statistically evaluated using the R^2, the bias and the RMSE, the last two defined by Equations (8) and (9).

$$\text{Bias} = \frac{1}{n}\sum_{i=1}^{n} \left(\text{SMC}_{\text{retrieved},i} - \text{SMC}_{\text{measured},i}\right) \quad (8)$$

$$\text{RMSE} = \sqrt{\left(\text{Bias}^2 + \text{Stddev}^2\right)} \quad (9)$$

where *Stddev* is the standard deviation; *i* refers to each one of the *n* samples; *measured* refers to the SMC measured in laboratory or in field conditions; and *retrieved* refers to the SMC value obtained from the SMC retrieval methods explained in Sections 3.1 and 3.2.

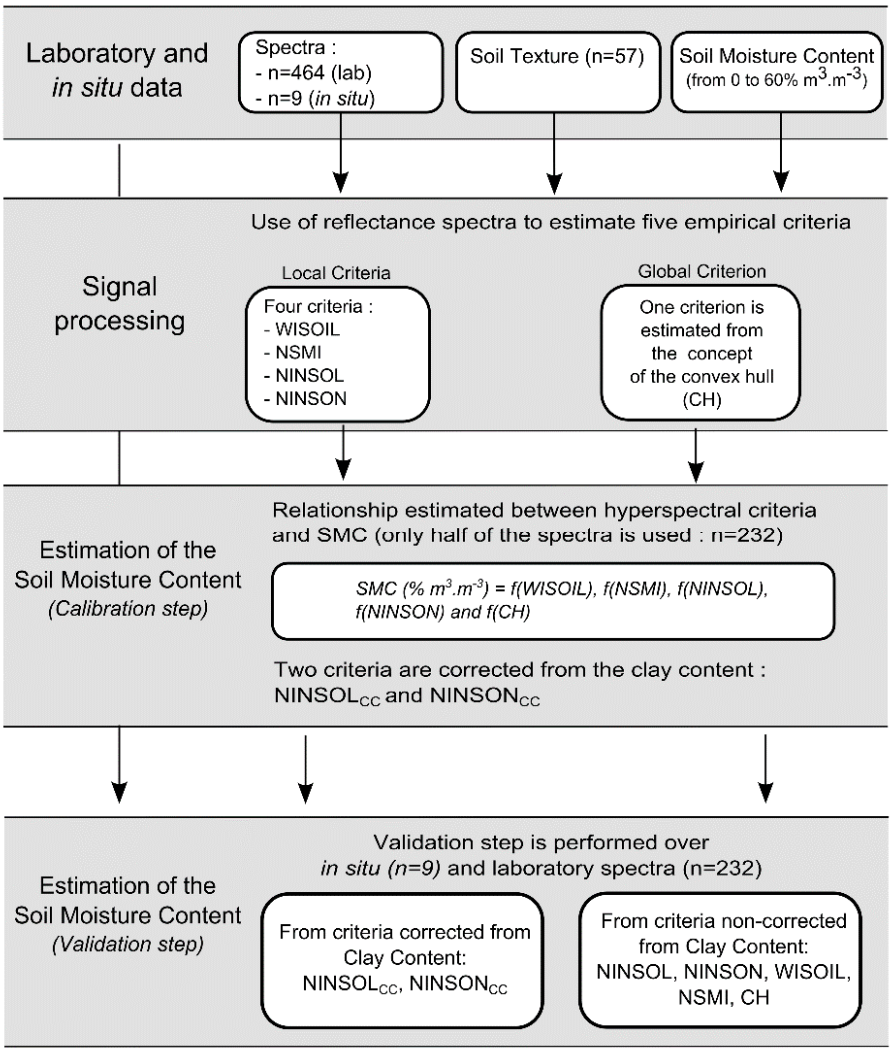

Figure 5. Flowchart showing the different methods used to estimate the volumetric soil moisture content from hyperspectral spectra.

3.1. Local Criteria to Retrieve SMC from Reflectance Spectrum

The local criteria are associated to spectral indices built from the soil spectral reflectance [35]. These indices are fitted with the samples SMC in order to provide an empirical law which links both parameters. In the literature this regression is established as linear or non-linear according to the index and the performance of the method is measured by the coefficient of determination [24,35,37,57]. Four indices were evaluated in this paper: WISOIL, NSMI, NINSOL and NINSON.

The WISOIL index was introduced by [58] and named by [24]. It is a ratio-based index (see Equation (10)) between the reflectance at a strong water absorption band ($\rho_{\lambda i}$, with λ_i = 1.45 μm) and the reflectance at weak water absorption band ($\rho_{\lambda j}$, with λ_j = 1.300 μm).

$$X_{\text{ratio}}(\lambda_i, \lambda_j) = \frac{\rho_{\lambda \text{i}}}{\rho_{\lambda \text{j}}} \tag{10}$$

Bryant *et al*. [24] showed that this index was linearly correlated with the SMC for three different soils: a light colored sandy loam Entisol, a red colored clay and iron rich Ardisol, and a dark colored silt/loam Mollisol (according to the nomenclature in the soil taxonomy developed by the Unites States Department of Agriculture), obtaining, respectively, a coefficient of determination of 0.76, 0.88 and 0.96.

The three other studied indices are normalized indices (see Equation (11)): the NSMI introduced by [37]; and the Normalized Index of NSWIR domain for SMC estimation from Linear correlation (NINSOL) and the Normalized Index of NSWIR domain for SMC estimation from Non Linear correlation (NINSON) both from [35].

$$X_{\text{norm}}(\lambda_i, \lambda_j) = \frac{\rho_{\lambda \text{i}} - \rho_{\lambda \text{j}}}{\rho_{\lambda \text{i}} + \rho_{\lambda \text{j}}} \tag{11}$$

For these indices, the wavelength pair (λ_i, λ_j), which give higher coefficient of determination between the index and the SMC, were determined by a regression matrix. The regression between the index and SMC_g is linear for the NSMI and NINSOL cases, and it is considered non-linear for the NINSON one. Table 2 shows the wavelengths and coefficient of determination for each normalized index.

Table 2. Summary of statistical performance of each normalized index as considered in [35], 2014. The most suitable couple of wavelengths to estimate soil moisture content are mentioned (λ_i, λ_j).

Index	λ_i (μm)	λ_j (μm)	Type of Regression Function	R^2
NSMI	1.80	2.12	Linear	0.61
NINSOL	2.08	2.23	Linear	0.87
NINSON	2.12	2.23	Non-linear	0.87

Figure 6 summarizes the wavelengths used by each index, superimposed with the atmospheric transmittance of a typical mid latitude summer atmosphere, and with a typical spectra of a bare soil surface (SMC = 28% $m^3 \cdot m^{-3}$, clay = 30%, sand = 40% and silt = 30%). The first wavelength of the WISOIL and NSMI index are placed nearby the water absorption bands of the atmosphere (transmittance trends to 0), so the performance of those indices could be affected by the noisy signal usually detected in these spectral regions. The two others indices (NINSOL and NINSON) are not affected by the specific water absorption bands of the atmosphere.

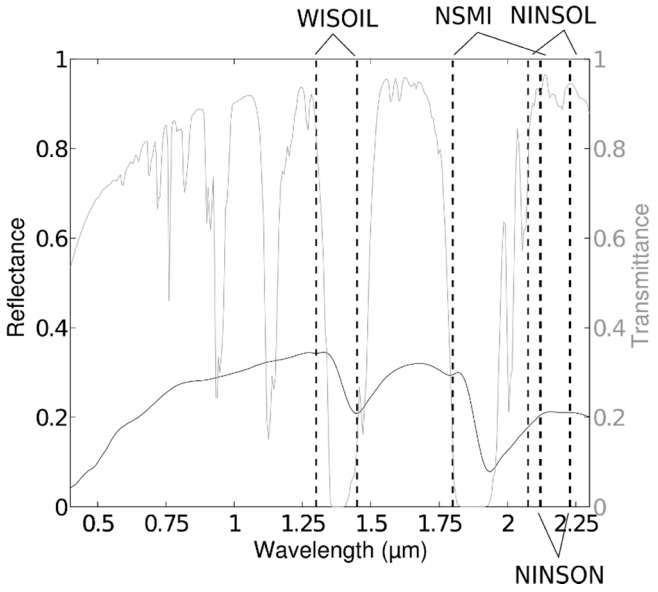

Figure 6. Example of a bare soil sample reflectance spectrum, superimposed with the index bands located by vertical dotted lines and with the atmospheric transmittance (in gray).

3.2. Global Criteria to Retrieve SMC from Reflectance Spectrum

The global criteria refer to estimate the SMC from a large continuous part of the surface spectral signature. In this paper, the used criterion is based on the convex hull (CH) adapted to the general shape of the natural logarithm of the reflectance spectrum from a triangular Delauney interpolation [35]. The process consists in:

(1) Generating hull points along the spectrum, excluding the absorption regions of water, clay, other minerals and organic matter,
(2) Calculating the area between the spectrum curve (its natural logarithm) and the CH (see Figure 7 for an example of the CH). This area increases with the SMC because of the presence of the water absorption bands. In these regions the value of the reflectance decreases when the SMC increases and as a consequence, the area between the spectrum and the CH increases,
(3) Estimating the SMC from the area previously calculated, by linking them with a linear regression.

4. Results and Discussions

4.1. SMC Retrieval: Calibration Step

Global and local criteria were calibrated using 232 spectra of laboratory reference database (representing 50% of the database spectra). The robustness of estimated model parameter values was tested by calibrating the models with the other 50% spectra. Equivalent model parameters values were obtained in both, which proved the parameter stability regardless of the spectra used in the calibration stage.

Figure 8 shows the results of the calibration step for the five criteria with their model fits and R^2. Each point on this figure corresponds to a sample and was associated to a color according to its CC. The calibration performance showed that all methods offered good performance, with R^2 ranging between 0.72 and 0.92. The lowest value was obtained for the NINSON index. The well-marked fits ($R^2 > 0.90$) were obtained for the WISOIL and the NSMI indices, and for the CH global criterion.

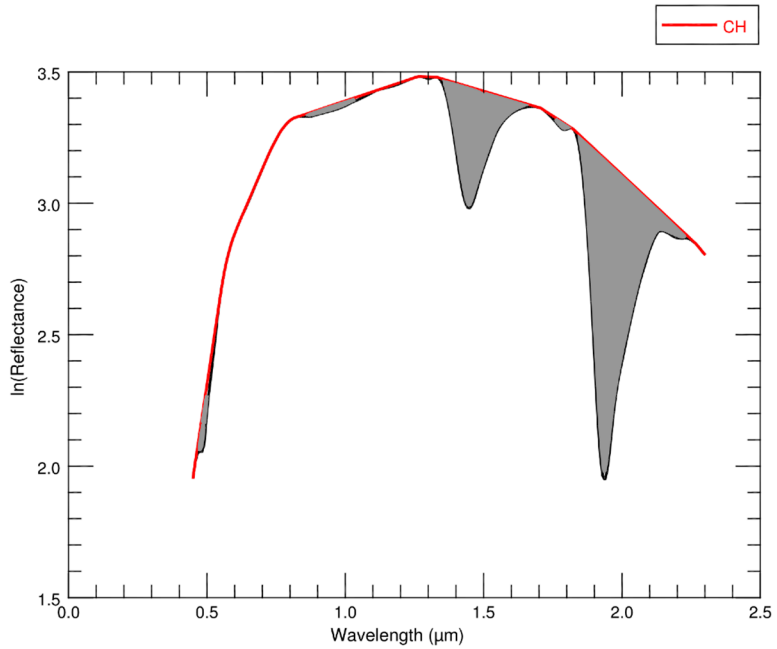

Figure 7. Example of a bare soil sample natural logarithm reflectance (black line) with its convex hull (red line). The area calculated between the spectrum curve and the CH is displayed in gray.

The CC did not affect the WISOIL, NSMI and CH criteria (Figure 8a,b,e). Only the NINSOL and NINSON indices have shown a well-marked dependency to CC values (Figure 8c,d). These two indices underestimated the SMC for samples with high CC and overestimated the SMC for samples with low CC. This phenomenon is explained by the use of the specific wavelength at 2.20 µm situated around the center of the clay absorption band [59]. This trend suggested that we could take into account the sample CC in order to improve the SMC retrieval. Regarding this assumption, we integrated the CC value in the NINSOL and NINSON indices. The bias for each CC value (*i.e.*, the mean difference between the retrieved SMC and the laboratory measured SMC for all the samples with the same CC value, see Equation (8)) was measured and linearly correlated with the CC (see Figure 9). The relations given by Equations (12) and (13) were obtained, with R^2 values around 0.8.

$$\text{Bias}_{\text{NINSOL}} = 10.08 - 0.33\text{CC} \qquad (R^2 = 0.78) \tag{12}$$

$$\text{Bias}_{\text{NINSON}} = 14.3 - 0.47\text{CC} \qquad (R^2 = 0.80) \tag{13}$$

Finally, we incorporated the relations 12 and 13 in the original NINSOL and NINSON models (shown in Figure 8c,d). The new SMC retrieval models, with the CC correction (SMC_{CC}) are, respectively, named $\text{NINSOL}_{\text{CC}}$ and $\text{NINSON}_{\text{CC}}$. They are defined, respectively, in Equations (14) and (15), and they allowed the estimation of SMC with a R^2 of 0.92 and 0.89, respectively .This meant an improvement of the data fit of 7% for the NINSOL and of 17% for the NINSON, after the CC correction.

$$\text{SMC}_{\text{CC}} = 4.92 - 255.34\text{NINSOL} + 0.33\text{CC} \tag{14}$$

$$\text{SMC}_{\text{CC}} = 11.48 - 495.33\text{NINSON} + 836.47\text{NINSON}^2 + 0.47\text{CC} \tag{15}$$

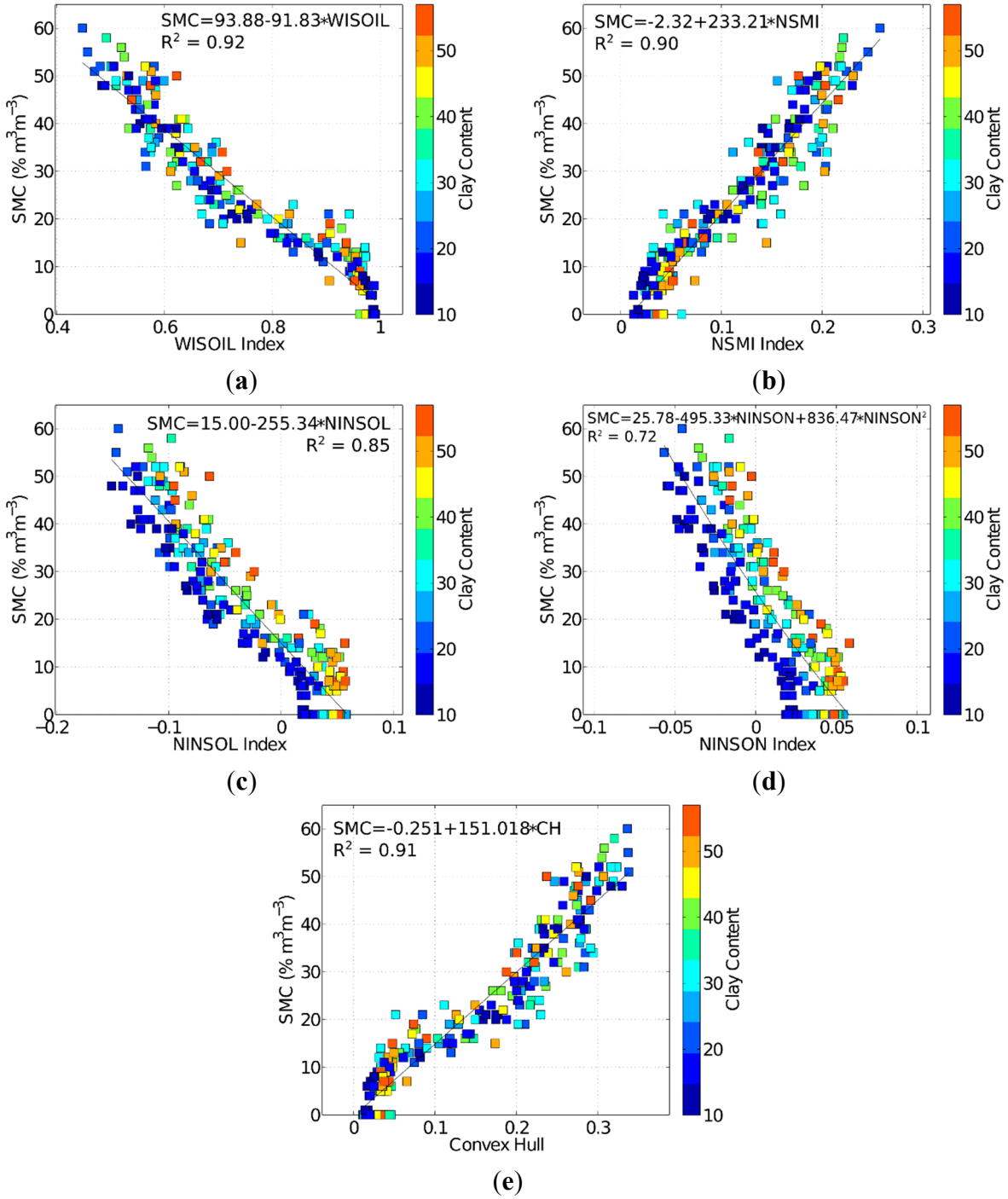

Figure 8. Comparison of the relationships estimated between measured soil moisture content and (**a**) WISOIL index; (**b**) NSMI index; (**c**) NINSOL index; (**d**) NINSON index and (**e**) the area between the spectra and the CH criteria. The colour bar indicates the clay content (%).

4.2. SMC Retrieval: Validation Step

In this section, the seven criteria were considered: WISOIL, NSMI, NINSOL, NINSOL$_{CC}$, NINSON, NINSON$_{CC}$ and CH. Two validation cases were tested depending on the origin of the spectra measurements: laboratory or *in-situ*.

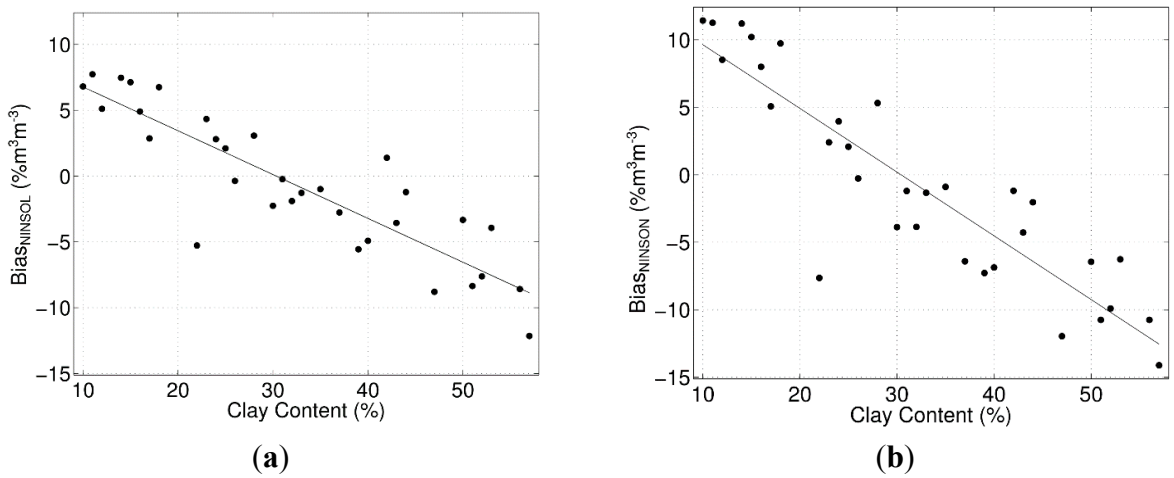

Figure 9. Relationships estimated between soil moisture content bias (Equation (8)) for each value of clay content, *versus* the clay content (see Equations (12) and (13)). For (**a**) NINSOL case and for (**b**) NINSON case.

4.2.1. From Laboratory Spectra

The validation of the models with the 232 validation spectra was done by comparing the retrieved SMC with the at-laboratory measured SMC. Results are shown in Figure 10 and in Table 3, with the statistical values defined by the Equations (8) and (9).

Table 3. Statistical performance from the validation of the models (n = 232 spectra have been used during the validation process).

Criteria	Bias (% m^3·m^{-3})	Stddev (% m^3·m^{-3})	RMSE (% m^3·m^{-3})	R^2
WISOIL	−0.1	4.8	4.8	0.92
NSMI	0.2	5.4	5.4	0.90
NINSOL	−0.2	6.1	6.1	0.87
NINSOL$_{CC}$	−0.7	4.9	5.0	0.92
NINSON	−0.3	8.3	8.3	0.76
NINSON$_{CC}$	−0.6	6.4	6.4	0.88
CH	0.0	5.1	5.1	0.91

All the criteria provided comparable results in terms of RMSE (between around 5% m^3·m^{-3} and 8% m^3·m^{-3}) and R^2 (between 0.77 and 0.92) and offered equivalent performance to retrieve SMC. Clay content dependence was no longer observed for the NINSOL$_{CC}$ and NINSON$_{CC}$ criteria (comparing with Figure 8c,d). Statistically, the CC correction ameliorated the NINSOL and NINSON results, with the decrease of RMSE of 1.1% m^3·m^{-3} and of 1.9% m^3·m^{-3}, respectively. The improvement of the error was linked with the decrease of the data dispersion, which is given by the standard deviation. Nevertheless, the bias increased after the CC correction due to the bias definition itself (Equation (8)): for NINSOL$_{CC}$ and NINSON$_{CC}$ the majority of the SMC values were underestimated, while for NINSOL and NINSON the points with a SMC overestimation compensated for the ones with an underestimation, obtaining a bias near to 0% m^3·m^{-3}. The latter was also the case for WISOIL, NSMI and CH criteria, whose biases were also near to 0% m^3·m^{-3}.

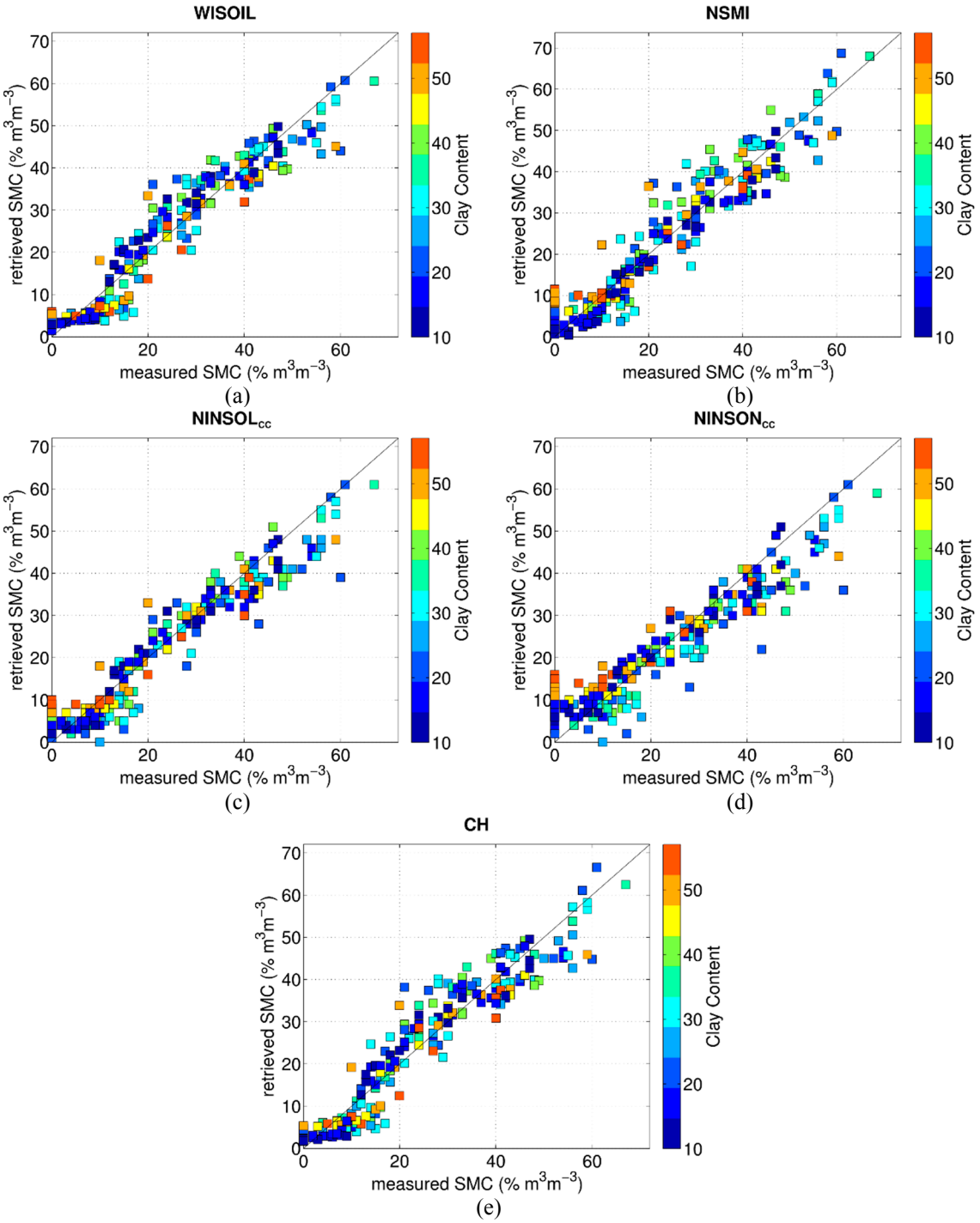

Figure 10. Comparison between measured and estimated SMC. Four criteria are considered: (**a**) WISOIL; (**b**) NSMI; (**c**) NINSOL$_{CC}$; (**d**) NINSON$_{CC}$ and (**e**) CH. The color bar indicates the clay content (%).

4.2.2. From *In-situ* Spectra

The SMC retrieval models defined in Section 4.1 were applied to the field database acquired over one parcel of the site of "Lamasquère" (Figure 1). A mean CC value of 46% was measured for the field area in a radius of 50 m around the ASD spectral measurements. Results of the comparison between the retrieved SMC values and the *in-situ* measured SMC values are shown in Figure 11 and statistics performance of global and local methods are summarized in Table 4.

Table 4. Statistical values computed from the comparison of the retrieved soil moisture content (SMC) and the *in-situ* measured SMC.

Criteria	Bias (% $m^3 \cdot m^{-3}$)	Stddev (% $m^3 \cdot m^{-3}$)	RMSE (% $m^3 \cdot m^{-3}$)	R^2
WISOIL	−4.7	4.7	6.6	0.90
NSMI	−6.4	5.5	8.5	0.87
NINSOL	−7.4	4.7	8.8	0.91
$NINSOL_{CC}$	−2.6	4.7	5.4	0.91
NINSON	−8.1	6.2	10.2	0.89
$NINSON_{CC}$	−0.8	6.2	6.2	0.89
CH	2.0	9.5	9.7	0.67

Figure 11c,d shows together the $NINSOL_{CC}$ and NINSOL ($NINSON_{CC}$ and NINSON) criteria. $NINSOL_{CC}$ and $NINSON_{CC}$ approaches introduce the CC information as an additive parameter (see Equations (12) and (13)). Thus, the CC correction introduced a bias to the estimated SMC but it did not change the slope. Moreover, the CC correction contributed to the decrease of the NINSOL and NINSON mean bias. As a result, the RMSE improved around 4% $m^3 \cdot m^{-3}$ which is twice the improvement obtained in laboratory conditions. The data dispersion was not affected by the CC correction because the nine *in-situ* samples considered had the same CC value.

Best results (lower RMSE and higher R^2) were achieved by $NINSOL_{CC}$, followed by $NINSON_{CC}$ and WISOIL. The CH method provided the weakest performance. NSMI was the medium option with average performance in comparison to the other methods.

Comparing the statistical results from laboratory data and the ones from field data, we observed that they were similar for the $NINSOL_{CC}$ and $NINSON_{CC}$ cases. Nevertheless the RMSE rose, respectively, around a 2% $m^3 \cdot m^{-3}$, a 3% $m^3 \cdot m^{-3}$ and 5% $m^3 \cdot m^{-3}$ for WISOIL, NSMI and CH criteria in field conditions. Moreover, the R^2 for the CH criterion was significantly lower than the R^2 for the field measurements. During *in-situ* measurements, a noisy signal due to the atmosphere was registered in the absorption bands and had to be approximated by a smoothing process in order to be able to construct the continuum used by the CH criterion to evaluate the area directly related to the SMC.

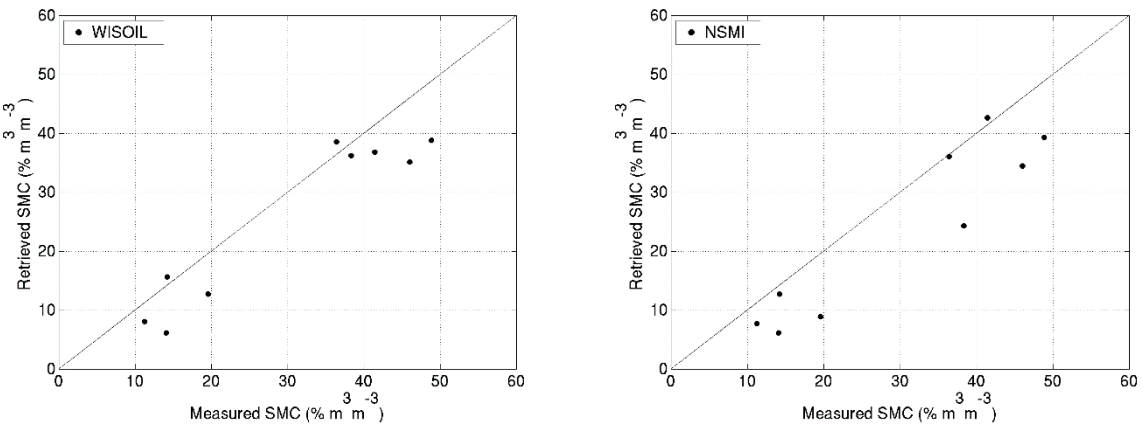

(**a**) (**b**)

Figure 11. *Cont.*

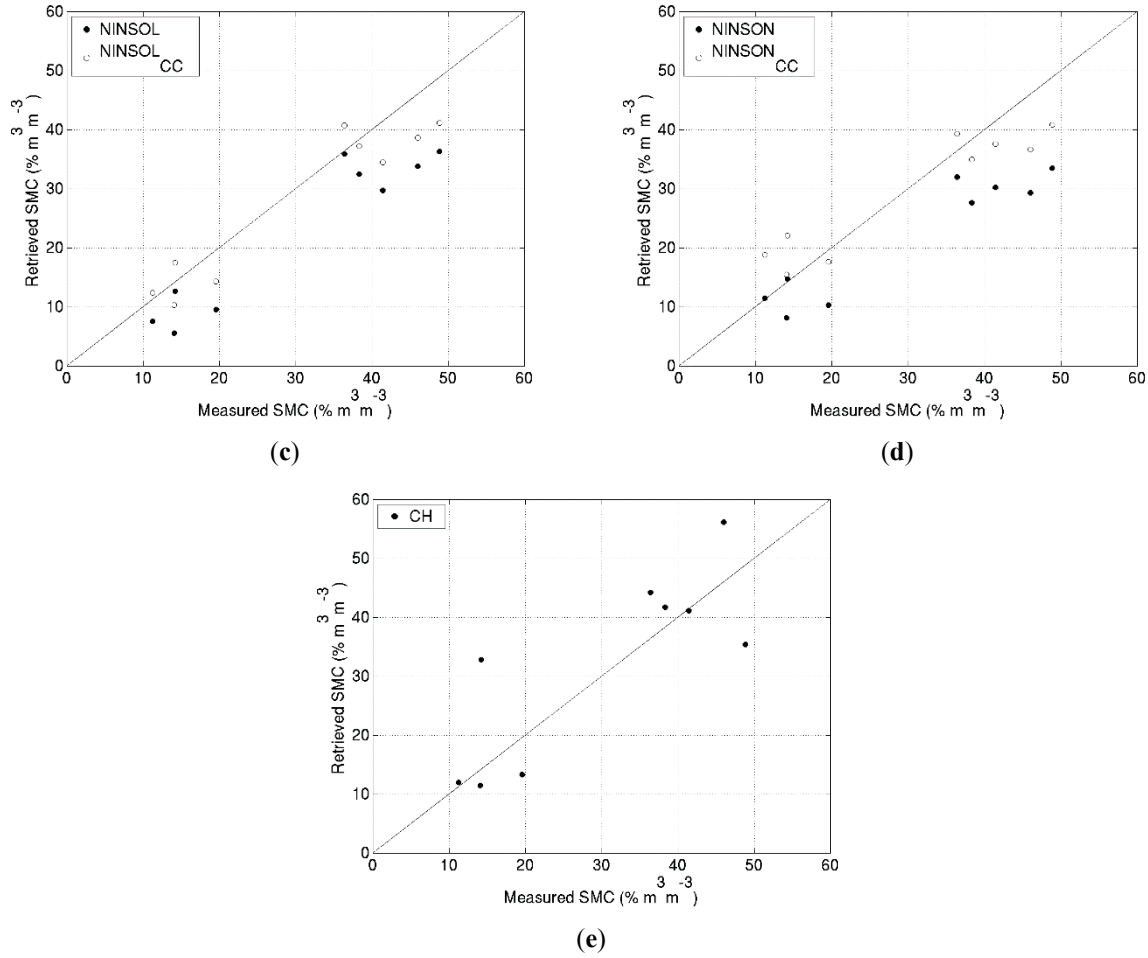

Figure 11. Retrieved soil moisture content (SMC) from each criteria fit *versus in-situ* measured SMC.

5. Conclusions and Perspectives

This study demonstrated the potential of hyperspectral approaches to estimate SMC over bare soil, and proposed an original method to take into account the CC of the soil to improve the estimation of the SMC. Five different criteria were tested to retrieve the SMC from the spectral reflectance. Four local indices (WISOIL, NSMI, NINSOL and NINSON) and one global criterion (CH) were evaluated.

These criteria were first calibrated using a reference database composed of 232 laboratory measurements (reflectance and SMC). The calibration step showed two important points: (1) the five criteria provided good statistical performance (R^2 between 0.7 and 0.92); and (2) the NINSOL and NINSON indices presented a dependence on the CC. This soil parameter was thus integrated in two new criteria: $NINSOL_{CC}$ and $NINSON_{CC}$.

The seven criteria were then validated first using laboratory data (232 reflectance spectra with their associated CC and SMC values) and finally with *in-situ* data (9 reflectance spectra with their associated CC and SMC values). In laboratory conditions, all criteria except NINSON obtained RMSE around 5% $m^3 \cdot m^{-3}$ and R^2 around 0.9. For the *in-situ* case, best results (RMSE < 7% $m^3 \cdot m^{-3}$ and R^2~0.9) were obtained for $NINSOL_{CC}$, $NINSON_{CC}$ and WISOIL. NSMI and CH were affected by the noisy signal introduced by the atmosphere in the water vapor absorption bands. Although the WISOIL spectral bands are situated nearby the water vapor absorption region at 1.4 μm (see Figure 6), the index performance was

not affected by spectral noise. Nevertheless, when coarser spectral resolutions will be considered, as in the case of airborne or spaceborne instruments, noisy signal is expected which would have a negative effect on the index SMC retrieval potential. NSMI performance outside laboratory conditions were poor due to the use of the bands in the atmospheric water vapor absorption region, that is in field conditions or in remote sensing imagery conditions. The CH criterion was not robust to outdoor measurements.

Results showed the interest of using the clay content information to improve the SMC retrieval in field conditions. Therefore, NINSOL$_{CC}$ and NINSON$_{CC}$ criteria can be potentially useful to obtain the SMC from optical remote sensing images. The inconvenient of NINSOL$_{CC}$ and NINSON$_{CC}$ criteria is the requirement of the *a priori* knowledge of CC. In this regard, a study of the impact of the CC accuracy over NINSOL$_{CC}$ and NINSON$_{CC}$ criteria should be done. On the one hand, if results show that these indices need accurate CC estimation, the CC could be predicted with local methods like PLSR [60,61]. In that case, NINSOL$_{CC}$ and NINSON$_{CC}$ will be used at the local scale for SMC estimation using airborne hyperspectral imagery. On the other hand, if the accuracy study shows that an error on the CC is accepted, CC might be deduced from geological cards and both indices will be applied at a global scale to satellite data. In any case, the impact of the spatial and spectral resolutions on the SMC retrieval should be studied to anticipate the indices performance under airborne and space-borne configurations.

Acknowledgments

The authors would like to thank Jean François Fayel for his help with the signal processing and for his energy during ground and laboratory measurements; Pierre-Yves Foucher and Emmanuelle Thouin for their help with field measurements. This work was funded by the project HUMPER-Mission HYPXIM, of the TOSCA-CNES program.

Author Contributions

All authors contributed equally to this work.

Conflicts of Interest

The authors declare no conflict of interest.

References

1. Chen, X.; Zhang, Z.C.; Chen, X.H.; Shi, P. The impact of land use and land cover changes on soil moisture and hydraulic conductivity along the karst hill slopes of southwest China. *Environ. Earth Sci.* **2009**, *59*, 811–820.
2. Munroa, R.K.; Lyonsa, W.F.; Shao, Y.; Wood, M.S.; Hood, L.M.; Leslie, L.M. Modeling land surface atmosphere interactions over the Australian continent with an emphasis on the role of soil moisture. *Environ. Model. Softw.* **1998**, *13*, 333–339.
3. Chen, L.; Wang, J.; Wei, W.; Fu, B.; Wu, D. Effects of landscape restoration on soil water storage and water use in the Loess Plateau Region, China. *For. Ecol. Manag.* **2010**, *259*, 1291–1298.
4. Ahmad, S.; Kalra, A.; Stephen, H. Estimating soil moisture using remote sensing data: A machine learning approach. *Adv. Water Resour.* **2010**, *33*, 69–80.

5. Watson, R.; Moss, R.; Zinyower, M. *The Regional Impacts of Climate Change: An Assessment of Vulnerability*; IPCC Special Report; Cambridge University: Cambridge, UK, 1998.
6. Shao, Y.; Henderson-Sellers, A. Modeling soil moisture: A project for intercomparison of land surface parameterization schemes phase 2(b). *J. Geophys. Res.* **1996**, *101*, 7227–7250.
7. De Roo, A.P.J.; Offermans, R.J.E.; Cremers, N.H.D.T. LISEM a single-event physically based hydrological and soil erosion model for drainage basins II: Sensitivity analysis, validation and application. *Hydrol. Process.* **1998**, *10*, 1119–1126.
8. Merritt, W.; Letcher, R.; Jakeman, A. A review of erosion and sediment transport models. *Environ. Model. Softw.* **2003** *18*, 761–799.
9. Hively, W.D.; McCarty, G.W.; Reeves, J.B.; Lang, M.W.; Oesterling, R.A.; Delwiche, S.R. Use of airborne hyperspectral imagery to map soil properties in tilled agricultural fields. *Appl. Environ. Soil Sci.* **2011**, *2011*, doi:10.1155/2011/358193.
10. Ben-Dor, E.; Chabrillat, S.; Demattê, J.A.M.; Taylor, G.R.; Hill, J.; Whiting, M.L.; Sommer, S. Using imaging spectroscopy to study soil properties. *Remote Sens. Environ.* **2009**, *113*, 538–555.
11. Nocita, M.; Stevens, A.; Noon, C.; Wesemae, B.V. Prediction of soil organic carbon for different levels of soil moisture using Vis-NIR spectroscopy. *Geoderma* **2013**, *199*, 37–42.
12. Fu, B.J.; Wang, J.; Chen, L.D.; Qiu, Y. The effects of land use on soil moisture variation in the Danangou catchment of the Loess Plateau, China. *Catena* **2003**, *54*, 197–213.
13. Knapp, A.K.; Fay, P.; Blair, J.; Collins, S.; Smith, M.; Carlisle, J.; Harper, C.; Danner, B.; Lett, M.; McCarron, J. Rainfall variability, carbon cycling, and plant species diversity in a mesic grassland. *Science* **2002**, *298*, 2202–2205.
14. Kanamitsu, M.; Lu, C.H.; Schemm, J.; Ebisuzaki, W. The predictability of soil moisture and near-surface temperature in hindcasts of the NCEP seasonal forecast model. *J. Clim.* **2003**, *16*, 510–521.
15. Zhang, W.J.; Lu, Q.F.; Gao, Z.Q.; Peng, J. Response of remotely sensed normalized difference water deviation index to the 2006 drought of eastern Sichuan Basin. *Sci. China Ser. D Earth Sci.* **2008**, *51*, 748–758.
16. Muller, E.; Decamps, H. Modeling soil moisture reflectance. *Remote Sens. Environ.* **2000**, *76*, 173–180.
17. Prasad, A.K.; Chaib, L.; Singh, R.P.; Kafatos, M. Crop yield estimation model for Iowa using remote sensing and surface parameters. *Int. J. Appl. Earth Obs. Geoinf.* **2006**, *8*, 26–33.
18. Nanni, M.R.; Dematte, J.A.M. Spectral reflectance methodology in comparison to traditional soil analysis. *Soil Sci. Soc. Am. J.* **2006**, *70*, 393–407.
19. Hadria, R.; Duchemin, B.; Jarlan, L.; Dedieu, G.; Baup, F.; Khabba, S.; Olioso, A.; Le Toan, T. Potentiality of optical and radar satellite data at high spatio-temporal resolutions for the monitoring of irrigated wheat crops in Morocco. *Int. J. Appl. Earth Obs. Geoinf.* **2010**, *12*, S32–S37.
20. Yanmin, Y.; Na, W.; Youqi, Ch.; Yingbin, H.; Pengqin, T. Soil moisture monitoring using hyper-spectral remote sensing technology. In Proceedings of the Second IITA International Conference on Geoscience and Remote Sensing (IITA-GRS 2010), Qingdao, China, 28–31 August 2010; pp. 373–376.
21. Vauclin, M. L'humidité des sols en hydrologie: Intérêt et limites de la télédétection. In *Hydrological Applications of Remote Sensing and Remote Data Transmission*, Proceedings of the Hamburg Symposium, August 1983; IAHS publisher: Wallingford, UK; pp. 401–409. Available online: https://www.itia.ntua.gr/hsj/redbooks/145/iahs_145_0499.pdf (accessed on 19 March 2015).

22. Nduwamungu, C.; Ziadi, N.; Tremblay, G.F.; Parent, L.E. Near-infrared reflectance spectroscopy prediction of soil properties: Effects of sample cups and preparation. *Soil Sci. Soc. Am. J.* **2009**, *73*, 1896–1903.
23. Yang, Z.P.; Ouyang, H.; Zhang, X.Z.; Xu, X.G.; Zhou, C.; Yang, W. Spatial variability of soil moisture at typical alpine meadow and steppe sites in the Qinghai-Tibetan Plateau permafrost region. *Environ. Earth Sci.* **2011**, *63*, 477–488.
24. Bryant, R.; Thoma, D.; Moran, S.; Holifield, C.; Goodrich, D.; Deefer, T.; Paige, G.; Williams, D.; Skirvin, S. Evaluation of hyperspectral, infrared temperature and radar measurements for monitoring surface soil moisture. In Proceedings of the First Interagency Conference on Research in the Watersheds, Benson, AZ, USA, 27–30 October 2003; pp. 528–533.
25. Wagner, W.; Bloshl, G.; Pampaloni, P.; Calvet, J.C.; Bizzarri, B.; Wigneron, J.P.; Kerr, Y. Operational readiness of microwave remote sensing of soil moisture for hydrologic applications. *Nord. Hydrol.* **2007**, *38*, 1–20.
26. Kerr, Y.H.; Waldteufel, P.; Wigneron, J.P.; Martinuzzi, J.M.; Font, J.; Berger, M. Soil moisture retrieval from space: The Soil Moisture and Ocean Salinity (SMOS) mission. *IEEE Trans. Geosci. Remote Sens.* **2001**, *39*, 1729–1735.
27. Stamenkovic, J.; Tuia, D.; de Morsier, F.; Borgeaud, M.; Thiran, J.P. Estimation of soil moisture from airborne hyperspectral imagery with support vector regression. In Proceedings of the Workshop on Hyperspectral Image and Signal Processing: Evolution in Remote Sensing (WHISPERS), Lausanne, Switzerland, 25–27 June 2014.
28. Peng, J.; Shen, H.; He, S.W.; Wu, J.S. Soil moisture retrieving using hyperspectral data with the application of wavelet analysis. *Environ. Earth Sci.* **2012**, *69*, 279–288.
29. Kaleita, A.L.; Tian, L.F.; Hirschi, M.C. Relationship between soil moisture content and soil surface reflectance. *Trans. Am. Soc. Agric. Eng.* **2005**, *48*, 1979–1986.
30. Angström, A. The albedo of various surfaces of ground. *Geogr. Ann.* **1925**, *7*, 323–327.
31. Bach, H.; Mauser, W. Modelling and model verification of the spectral reflectance of soils under varying moisture conditions. In Proceedings of the Geoscience and Remote Sensing Symposium (IGARSS), Pasadena, CA, USA, 8–12 August 1994; Volume 4, pp. 2354–2356.
32. Liu, W.; Baret, F.; Gu, X.F.; Tong, Q.; Zheng, L.; Zhang, B. Relating soil surface moisture to reflectance. *Remote Sens. Environ.* **2002**, *81*, 238–246.
33. Lesaignoux, A.; Fabre, S.; Briottet, X. Influence of soil moisture content on spectral reflectance of bare soils in the 0.4–14 m domain. *Int. J. Remote Sens.* **2013**, *34*, 2268–2285.
34. Whiting, M.L.; Li, L.; Ustin, S.L. Predicting water content using gaussian model on soil spectra. *Remote Sens. Environ.* **2004**, *89*, 535–552.
35. Fabre, S.; Briottet, X.; Lesaignoux, A. Estimation of soil moisture content from the spectral reflectance of bare soils in the 0.4–2.5 μm domain. *Sensors* **2015**, *15*, 3262–3281.
36. Lobell, D.B.; Asner, G.P. Moisture effects on soil reflectance. *Soil Sci. Am. J.* **2002**, *66*, 722–727.
37. Haubrock, S.N.; Chabrillat, S.; Lemmnitz, C.; Kaufmann, H. Surface soil moisture quantification models from reflectance data under field conditions. *Int. J. Remote Sens.* **2008**, *29*, 3–29.
38. Hummel, J.W.; Sudduth, K.A.; Hollinger, S.E. Soil moisture and organic matter prediction of surface and subsurface soils using an NIR soil sensor. *Comput. Electron. Agric.* **2001**, *32*, 149–165.

39. Bruand, A.; Tessier, D. Water retention properties of the clay in soils developed on clayey sediments: Significance of parent material and soil history. *Eur. J. Soil Sci.* **2000**, *51*, 679–688.
40. Stevens, A.; Udelhoven, T.; Denis, A.; Tychon, B.; Lioy, R.; Hoffman, L.; van Wesemael, B. Measuring soil organic carbon in croplands at regional scales using imaging spectroscopy. *Geoderma* **2010**, *158*, 32–45.
41. Mulder, V.L.; de Brui, S.; Schaepman, M.E.; Mayr, T.R. The use of remote sensing in soil and terrain mapping—A review. *Geoderma* **2011**, *162*, 1–19.
42. Haubrock, S.; Chabrillat, S.; Kaufmann, H. Application of hyperspectral imaging for the quantification of surface soil moisture in erosion monitoring and modeling. In Proceedings of the 4th EARSel Workshop on Imaging Spectroscopy, Warsaw, Poland, 27–30 April 2005.
43. Finn, M.P.; Lewis, M.; Bosch, D.D.; Giraldo, M.; Yamamoto, K.; Sullivan, D.G.; Kincaid, R.; Luna, R.; Allam, G.K.; Kvien, C. Remote sensing of soil moisture using airborne hyperspectral data. *GISci. Remote Sens.* **2011**, *48*, 522–540.
44. Sobrino, J.A.; Franch, B.; Mattar, C.; Jiménez-Muñoz, J.C.; Corbari, C. A method to estimate soil moisture from Airborne Hyperspectral Scanner (AHS) and ASTER data: Application to SEN2FLEX and SEN3EXP campaigns. *Remote Sens. Environ.* **2012**, *117*, 415–428.
45. Wang, Q.; Li, P.; Zhi, P.; Chen, X. Calibration and validation of salt-resistant hyperspectral indices for estimating soil moisture in arid land. *J. Hydrol.* **2011**, *408*, 276–285.
46. Haubrock, S.; Chabrillat, S.; Kuhnert, M.; Hostert, P.; Kaufmann, H. Surface soil moisture quantification and validation based on hyperspectral data and field measurements. *J. Appl. Remote Sens.* **2008**, *2*, doi:10.1117/1.3059191.
47. Lopinto, E.; Ananasso, C. The Prisma Hyperspectral Mission. In proceedings of the 33rd EARSeL Symposium Towards Horizon 2020: Earth Observation and Social Perspectives, Matera, Italy, 3–6 June 2013.
48. EnMAP. Available online: http://www.enmap.org/ (accessed on 27 March 2014).
49. Michel, S.; Lefevre-Fonollosa, M.-J.; Hosford, S. HYPXIM—A hyperspectral satellite defined for science, security and defence users. In Proceedings of the Hyperspectral Workshop, ESA-Esrin Frascati, Italy, 17–19 March 2010.
50. Baup, F.; Fieuzal, R.; Marais-Sicre, C.; Dejoux, J.-F.; Le Dantec, V.; Mordelet, P.; Claverie, M.; Hagolle, O.; Lopes, A.; Keravec, P.; *et al.* MCM'10: An experiment for satellite multi-sensors crop monitoring. From high to low resolution observations. In Proceedings of the Geoscience and Remote Sensing Symposium (IGARSS), Munich, Germany, 22–27 July 2012; pp. 4849–4852.
51. Béziat, P.; Ceschia, E.; Dedieu, G. Carbon balance of a three crop succession over two cropland sites in South West France. *Agric. For. Meteorol.* **2009**, *149*, 1628–1645.
52. Dejoux, J.-F.; Dedieu, G.; Hagolle, O.; Ducrot, D.; Menaut, J.-C.; Ceschia, E.; Baup, F.; Demarez, V.; Marais-Sicre, C.; Kadiri, M.; *et al.* Kalideos OSR MiPy: Un observatoire pour la recherche et la démonstration des applications de la télédétection a la gestion des territoires. *Rev. Fr. Photogramm. Télédétect.* **2012**, *197*, 17–30.
53. Marais-Sicre, C.; Baup, F.; Fieuzal, R. Determination of the crop row orientations from Formosat-2 multi-temporal and panchromatic images. *ISPRS J. Photogramm. Remote Sens.* **2014**, *94*, 127–142.
54. Gaskin, G.J.; Miller, J.D. Measurement of soil water content using a simplified impedance measuring technique. *J. Agric. Eng. Resour.* **1996**, *63*, 153–160.

55. European Soil Bureau working group. "HYdraulic PRoperties of European Soils" (HYPRES). Texture Classes. HYPRES Website. Available online: http://www.macaulay.ac.uk/hypres/hypressoil.html (accessed on 29 January 2015).
56. Dorigo, W.; Bachmann, M.; Heldens, W. *AS Toolbox and Processing of Field Spectra, User's Manual*; German Aerospace Center (DLR): Wessling, Germany, December 2006; Version 1.13.
57. Khanna, S.; Palacios-Orueta, A.; Whiting, M.L.; Ustin, S.L.; Riao, D.; Litago, J. Development of angle indexes for soil moisture estimation, dry matter detection and land-cover discrimination. *Remote Sens. Environ.* **2007**, *109*, 154–165.
58. Whalley, W.R.; Leeds-Harrison, P.B.; Bowman, G.E. Estimation of soil moisture status using near infrared reflectance. *Hydrol. Process.* **1991**, *5*, 321–327.
59. Crowley, J.K.; Brickey, D.W.; Rowan, L.C. Airborne imaging spectrometer data of the Ruby Mountains, Montana: Mineral discrimination using relative absorption band-depth images. *Remote Sens. Environ.* **1989**, *29*, 121–134.
60. Wold, S.; Sjöström, M.; Eriksson, L. PLS-regression: A basic tool of Chemometrics. *Chemom. Intell. Lab. Syst.* **2001**, *58*, 109–130.
61. Gomez, C.; Lagacherie, P.; Coulouma, G. Regional predictions of eight common soil properties and their spatial structures from hyperspectral VIS-NIR data. *Geoderma* **2012**, *189*, 176–185.